HHS Public Access

Author manuscript

Mol Cancer Ther. Author manuscript; available in PMC 2015 July 28.

Published in final edited form as:

Mol Cancer Ther. 2008 December ; 7(12): 3878–3888. doi:10.1158/1535-7163.MCT-08-0476.

In vivo characterization of a polymeric nanoparticle platform with potential oral drug delivery capabilities

Savita Bisht[1], **Georg Feldmann**[1], **Jan-Bart M. Koorstra**[1,5], **Michael Mullendore**[1], **Hector Alvarez**[1], **Collins Karikari**[1], **Michelle A. Rudek**[2], **Carlton K. Lee**[2,3], **Amarnath Maitra**[4], and **Anirban Maitra**[1]

[1]Department of Pathology, Johns Hopkins University School of Medicine, Baltimore, Maryland [2]Department of Oncology, Johns Hopkins University School of Medicine, Baltimore, Maryland [3]Department of Pediatrics, The Sol Goldman Pancreatic Cancer Research Center, Johns Hopkins University School of Medicine, Baltimore, Maryland [4]Department of Chemistry, University of Delhi, Delhi, India [5]Department of Pathology, University Medical Center Utrecht, Utrecht, the Netherlands

Abstract

Nanotechnology has enabled significant advances in the areas of cancer diagnosis and therapy. The field of drug delivery is a sterling example, with nanoparticles being increasingly used for generating therapeutic formulations of poorly water-soluble, yet potent anticancer drugs. Whereas a number of nanoparticle-drug combinations are at various stages of preclinical or clinical assessment, the overwhelming majorities of such systems are injectable formulations and are incapable of being partaken orally. The development of an oral nano-delivery system would have distinct advantages for cancer chemotherapy. We report the synthesis and physicochemical characterization of orally bioavailable polymeric nanoparticles composed of *N*-isopropylacrylamide, methylmethacrylate, and acrylic acid in the molar ratios of 60:20:20 (designated NMA622). Amphiphilic NMA622 nanoparticles show a size distribution of <100 nm (mean diameter of 80 ± 34 nm) with low polydispersity and can readily encapsulate a number of poorly water-soluble drugs such as rapamycin within the hydrophobic core. No apparent systemic toxicities are observed in mice receiving as much as 500 mg/kg of the orally administered void NMA622 for 4 weeks. Using NMA622-encapsulated rapamycin ("nanorapamycin") as a prototype for oral nano-drug delivery, we show favorable *in vivo* pharmacokinetics and therapeutic efficacy in a xenograft model of human pancreatic cancer. Oral nanorapamycin leads to robust inhibition of the mammalian target of rapamycin pathway in pancreatic cancer xenografts, which is accompanied by significant growth inhibition ($P < 0.01$) compared with control tumors. These data indicate that NMA622 nanoparticles provide a suitable platform for oral delivery of water-insoluble drugs like rapamycin for cancer therapy.

Requests for reprints: Anirban Maitra, Department of Pathology; Johns Hopkins University School of Medicine, CRB2, Room 345, 1550 Orleans Street, Baltimore, MD 21231. Phone: 410-955-3511; Fax: 410-614-0671. amaitra1@jhmi.edu.
S. Bisht and G. Feldmann contributed equally to this work.

Disclosure of Potential Conflicts of Interest

Johns Hopkins University has a patent pending (USPTO 20080107749). The authors disclosed no other potential conflicts of interest.

Introduction

Systemic delivery of poorly water-soluble (hydrophobic) drugs remains a major problem in clinical pharmacology. In the WHO Model List of Essential Medicines, as many as 25% of drugs are considered poorly water-soluble, using the Food and Drug Administration Biopharmaceutics Classification System for drug solubility (1). The conventional excipients used for solubilizing these agents [e.g., Cremophor EL, Tween (polysorbate)-80, etc.] can, in turn, lead to incidental adverse effects, including acute hypersensitivity reactions, fluid retention, and peripheral neuropathy (2, 3). The hunt for "solvent-free" formulations for commonly used hydrophobic drugs has led to the development of nanoparticle and liposomal drug delivery platforms, many of which have either been approved for clinical use (e.g., Abraxane, DaunoXome, or Doxil) or are undergoing evaluation in clinical trials (reviewed in ref. 4). Of note, the vast majorities of these improved formulations are administered i.v. and are not suitable for oral delivery.

Multiple lines of evidence suggest that cancer patients prefer the increased convenience, home-based administration, and "pill" formulation of orally administered regimens than that of parenteral drugs (5, 6). In some of these randomized trials, oral delivery was also associated with a decreased incidence of drug-related adverse effects, without compromising on efficacy (5, 6). Although concerns have been raised about potential nonadherence to oral regimens, more recent meta-analysis data suggest that oral chemotherapy is a reliable option for patients with solid tumors, both in the metastatic and adjuvant settings (reviewed in ref. 7). Cost-benefit reports of oral chemotherapy in the United States and elsewhere are scant; however, studies analyzing cost effectiveness of oral versus traditional i.v. regimens for colorectal cancer in Europe and Canada suggest significant savings with the former route, even with the higher individual costs for the new orally delivered drugs (8).

Here we report the synthesis and *in vivo* characterization of polymeric nanoparticles capable of systemic drug delivery through the oral route. Rapamycin (sirolimus), a macrolide used in the setting of transplantation as an immunosuppressant, has more recently been shown to be a potent anticancer agent in a variety of solid tumor models (9). Rapamycin is an inhibitor of the mammalian target of rapamycin (mTOR) pathway, which has a physiologic role in protein synthesis and cap-dependent translation, but can facilitate tumorigenesis and angiogenesis on aberrant activation (10). In addition, the mTOR pathway contributes to resistance toward common chemotherapeutic agents (e.g., microtubule inhibitors, platinum compounds, and tyrosine kinase inhibitors) through induction of cell survival pathways, and therapeutic synergy between rapamycin and many of these aforementioned drugs is demonstrable on combinatorial therapy (11, 12). Although a promising anticancer agent with favorable toxicity profile, rapamycin is a prototype for a poorly water-soluble, hydrophobic drug with low oral bioavailability (13). We report the favorable pharmacokinetic profile and therapeutic efficacy of an orally bioavailable polymeric nanoparticle encapsulated formulation of rapamycin ("nanorapamycin") and show the overall utility of our platform for *in vivo* drug delivery through the oral route.

Materials and Methods

Synthesis of NMA622 and NVA622 Polymeric Nanoparticles

A copolymer of *N*-isopropylacrylamide and acrylic acid, with either methylmethacrylate or vinylpyrrolidone, was synthesized through free radical polymerization, as shown in the accompanying flowchart (Fig. 1A). *N*-Isopropylacrylamide, methylmethacrylate, vinylpyrrolidone, and acrylic acid were obtained from Sigma-Aldrich. *N*-Isopropylacrylamide was recrystallized with hexane; methylmethacrylate, vinylpyrrolidone, and acrylic acid were freshly distilled before use. Thereafter, the monomers *N*-isopropylacrylamide, methylmethacrylate, and acrylic acid (designated NMA622) or *N*-isopropylacrylamide, vinylpyrrolidone, and acrylic acid (designated NVA622) were dissolved in water in a 60:20:20 molar ratio, respectively. Polymerization was initiated with ammonium persulfate (Sigma) as an initiator in a nitrogen (N_2) atmosphere. Ferrous sulfate ($FeSO_4$; Sigma) was added to activate the polymerization reaction and also to ensure complete polymerization of the monomers. In a typical experimental protocol for NMA622 synthesis, 66.6 mg *N*-isopropylacrylamide, 19.4 μL freshly distilled methylmethacrylate, and 14.0 μL acrylic acid (also freshly distilled) were added to 10 mL of water. To cross-link the polymer chains, 30 μL of *N*,*N*′-methylene-bis-acrylamide (Sigma; 0.049 g/mL) were added to the aqueous solution of monomers. The dissolved oxygen was removed by passing nitrogen gas for 30 min. Thereafter, 15 μL of $FeSO_4$ (0.5% w/v) and 13 μL of ammonium persulfate (5% w/v) were added. In case of NVA622, the respective weights and volumes were *N*-isopropylacrylamide 65 mg, vinylpyrrolidone 21 μL, and acrylic acid 13.7 μL, $FeSO_4$ 20 μL, ammonium persulfate 20 μL (20% w/v), and TEMED 20 μL. Polymerization was done at 30°C for 24 h in a N_2s atmosphere. After the polymerization was complete, the total aqueous solution of polymer was subjected to dialysis for 6 to 8 h to remove any residual monomers. Dialysis was done using a Spectrapore cellulose membrane dialysis tubing (molecular weight cutoff, 12 kDa) with a repeated exchange of water every 2 h. The dialyzed solution was then lyophilized immediately to obtain a dry powder for subsequent use, which was easily redispersible in aqueous media.

Loading of Rapamycin in NMA622 or NVA622 Polymeric Nanoparticles

Rapamycin (sirolimus) was purchased from LC Laboratories. Rapamycin loading into polymeric nanoparticles was done using a postpolymerization method. In this process of loading, the drug is dissolved after the copolymer formation has taken place, and rapamycin is directly loaded into the hydrophobic core of nanoparticles by physical entrapment. Physical entrapment was carried out as follows: 100 mg of the lyophilized polymer were dispersed in 10 mL distilled water and stirred to reconstitute the micelles. Free rapamycin was dissolved in chloroform (1% w/v) and the drug dissolved in $CHCl_3$ was added to the nanoparticle solution slowly with low heating to evaporate the chloroform. Additional drug encapsulation was facilitated within the polymeric nanoparticles by constant vortexing and mild sonication in a Branson 5510 water bath sonicator (Process Equipment & Supply, Inc.). Compared with the turbid suspension observed with free rapamycin dispersed in water, nanorapamycin resulted in a transparent solution (Fig. 1B). The drug-loaded nanoparticles were then lyophilized to dry powder for subsequent use.

In vitro Release Kinetics of Nanorapamycin

A known amount of lyophilized polymeric nanoparticles (200 mg) encapsulating 6 mg of rapamycin was dispersed in 20 mL phosphate buffer at two different pH conditions ("neutral" at pH 7.4 and "acidic" at pH 5.0) and the solution was divided among 20 microfuge tubes (1 mL each). The tubes were kept in a thermostable water bath set at 37°C. Free rapamycin is completely insoluble in water; therefore, at predetermined intervals of time, the solution was centrifuged at 3,000 rpm for 5 min to separate the released (pelleted) rapamycin from the loaded nanoparticles. Thereafter, the released rapamycin was redissolved in 1 mL of ethanol and the absorbance was measured spectrophotometrically at 273 nm. The concentration of the released rapamycin was then calculated using a standard curve of rapamycin in ethanol. The percentage of rapamycin released was determined from the equation

$$\text{Release}(\%) = \frac{[\text{Rapamycin}]_{\text{rel}}}{[\text{Rapamycin}]_{\text{tot}}} \times 100$$

where $[\text{Rapamycin}]_{\text{rel}}$ is the concentration of released rapamycin collected at time *t*, and $[\text{Rapamycin}]_{\text{tot}}$ is the total amount of rapamycin initially entrapped in the nanoparticles.

In vivo Pharmacokinetics of Oral Nanorapamycin

All animal experiments were approved by the Animal Care and Use Committee of Johns Hopkins University and animals were maintained in accordance to the guidelines of the American Association of Laboratory Animal Care. A series of pharmacokinetic studies were done using the two available oral nano-encapsulated rapamycin formulations (NMA622 and NVA622) in non–tumor-bearing CD1 mice to determine the superior formulation for further *in vivo* studies.

Experiment 1—Three separate cohorts of four mice were given oral doses of free rapamycin dissolved in water ("control"), NMA622, or NVA622 at an equivalent dose of 15 mg/kg of the active compound. Blood samples were obtained at 2 h after dosing.

Experiment 2—To determine equitable systemic distribution of orally administered nanorapamycin, blood was obtained at 2 h after dosing by cardiac puncture and from the facial vein in three mice receiving a single dose of 15 mg/kg of nanorapamycin (NMA622).

Experiment 3—The objective of this study was to perform head-to-head pharmacokinetic comparison of the two oral nanorapamycin formulations (NM622 and NVA622), and further, to compare these to the available commercial oral rapamycin (Rapamune). Two independent cohorts of six mice were administered a single oral dose of NMA622 or NVA622, equivalent to 15 mg/kg of active compound, and a third cohort of mice was administered an equivalent dose of oral Rapamune (Wyeth Pharmaceuticals). Blood samples were obtained from all cohorts at 30 min and at 2, 4, 8, and 24 h for determining free rapamycin concentration. Pharmacokinetics data were analyzed by noncompartmental methods (WinNonlin Standard, version 3.1 software, Pharsight Corporation). Individual maximum serum concentration (Cp_{max}) and time to reach Cp_{max} (T_{max}) values at steady

state were obtained by visual inspection of the semilogrithmic plots of serum concentrations *versus* time. Area under the concentration versus time to infinity curve ($AUC_{0\text{-infinity}}$) was calculated by the log-linear trapezoidal method. The elimination rate constant (*z*) was determined from the slope of the terminal phase of the serum concentration versus time curve using uniform weight. The elimination half-life ($T_{1/2}$) was calculated as 0.693 divided by *z*. Standard equations for apparent volume of distribution (Vd/*F*) and total clearance (Cl/*F*) were used.

In vivo Toxicity Studies of Void NMA622 Polymeric Nanoparticles in Mice

To determine any incidental toxicities from longer-term administration of the polymeric nanoparticles, wild-type CD1 mice ($n = 4$ per treatment arm; 2 males, 2 females) were treated with 500 mg/kg per day of void (i.e., not loaded with drug) NMA622 nanoparticle solution via oral gavage. Mice were monitored daily for behavioral abnormalities, and total body weights were measured weekly. After 4 wk, the mice were euthanized and comprehensive necropsies with organ harvests done.

Generation of S.c. Pancreatic Cancer Xenografts and Oral NanorapamycinTherapy

S.c. pancreatic cancer xenografts were generated as described elsewhere, using Panc198, a low-passage human pancreatic cancer xenograft that is highly sensitive to the injectable rapamycin analogue temsirolimus (CCI-779; refs. 14, 15). To generate xenografted cohorts for drug treatment studies, freshly harvested Panc198 xenograft tissue was cut into cubes of ~1 mm^3 under sterile conditions. Fresh tumor chunks were then s.c. implanted bilaterally into the flanks of male CD1 nu/nu athymic mice. Three weeks after s.c. implantation, the xenograft tumor volumes were assessed using digital calipers as described elsewhere (16). Nine mice with bilateral xenografts were then randomized to receive either PBS p.o., oral nanorapamycin (NMA622 at an equivalent dose of 15 mg/kg of free drug), or oral Rapamune (15 mg/kg) for 4 wk via oral gavage, at three mice per arm. In the three remaining mice, only one flank tumor was engrafted, and these were randomly divided among the three arms. Thus, the final control and treatment cohorts each composed of seven Panc198 xenografts across four CD1 nu/nu mice. Tumor volumes and mouse body weights were measured weekly. Mice were euthanized at the end of treatment; organs and xenograft tumor tissues were harvested and preserved in 10% formalin solution for histology and immunohistochemical studies or snap-frozen for Western blot analysis.

Blood Sampling and Determination of Rapamycin Concentrations

Whole blood (300 μL) was collected using EDTA-coated Microvette CB300 capillary tubes (Braintree Scientific) and stored at −80 °C until use. Free rapamycin blood concentrations were determined in the laboratory of Dr. Frederick Smith (Children's Memorial Hospital, Chicago, IL) using a high-performance liquid chromatography-tandem mass spectrometer (Waters 2795 liquid chromatograph coupled to a Micromass Quattro Micro TMS) as described elsewhere (17, 18).

Free rapamycin concentrations in harvested xenograft tumor tissue samples were measured in the Johns Hopkins Pharmacology Analytical core facility. In brief, tumor tissue homogenates were prepared by diluting 1:10 (w/v) in human plasma before extraction using

acetonitrile-*n*-butylchloride (1:4, v/v) containing known quantities of benzylphenylurea as the internal standard. After liquid extraction and evaporation, the sample was dissolved in 100 μL of acetonitrile/water (50:50, v/v). The analytes were separated on a Waters X-Terra MS C18 (50 × 2.1 mm, 3.5 μm) column using a mobile phase consisting of acetonitrile/2 mmol/L ammonium acetate (70:30, v/v) containing 0.1% formic acid using isocratic flow at 0.15 mL/min for 7 min. Rapamycin was monitored by tandem mass spectrometry with electrospray positive ionization. Calibration curves were generated over the range of 5.5 to 2,200 ng/g for tissue.

Immunohistochemistry

Immunostaining was done on formalin-fixed paraffin-embedded tissue sections as described elsewhere (15) with slight modifications. Anti–phospho-p70 S6 kinase (Thr^{389}; 1A5) antibody (#9206, Cell Signaling Technology) was used at 1:200 and visualized using the PowerVision+Poly-HRP IHC kit (Immunovision Technologies) following the standard protocol. Slides were counterstained with Harris hematoxylin solution. For Ki-67 (MIB1) staining, anti-Ki67 primary antibody (clone K2, Ventana Medical Systems) was used in combination with a Ventana Benchmark Autostainer. Antigen retrieval was done in EDTA buffer (pH 9.0) for 16 min, and the incubation time with the primary antibody was 32 min. The reaction was developed and visualized with the iView Detection Kit (Ventana Medical Systems).

Western Blot Analysis

Western blot analysis for mTOR activation was done as previously described with some minor modifications (19). For protein detection, the following antibodies were used: phospho-p70 S6 kinase (#9206, Cell Signaling; 1:1,000), p70 S6 kinase (H-160, Santa Cruz Biotechnology; 1:200), and actin (I-19, Santa Cruz Biotechnology; 1:200).

Statistical Analysis

Two-tailed *t* test and Mann-Whitney *U* test were done using Prism version 5.01 (GraphPad Software, Inc.). $P < 0.05$ was regarded as statistically significant. Diagrams show means and SDs unless indicated otherwise.

Results

Synthesis and Characterization of NMA622 and NVA622 Polymeric Nanoparticles

Polymeric nanoparticles of *N*-isopropylacrylamide, methylmethacrylate, and acrylic acid (NMA622) or *N*-isopropylacrylamide, vinylpyrrolidone, and acrylic acid (NVA622) were synthesized by random copolymerization of the vinyl end groups present in amphiphilic monomers (Fig. 1). The copolymer formed showed an amphiphilic character with a hydrophobic inner core and a hydrophilic outer shell, the latter being composed of water-soluble moieties like amides and carboxylates that project from the monomeric units.

The formation of water-soluble copolymer was assessed by nuclear magnetic resonance spectroscopy. In Fig. 2A, we illustrate a typical ^{1}H nuclear magnetic resonance spectrum and chemical shift assignments of the copolymer formed, using NMA622 as an example.

The figure also displays the structures of the monomeric units, with the dashed line representing the vinyl end groups involved in polymerization. Polymerization is clearly indicated by the absence of proton resonance of vinyl end groups of the monomers. Resonance can be observed at the upfield region (δ = 1.2– 2.3 ppm), attributable to the saturated protons of the polymeric network. The broad resonance peak at δ 0.8 to 1.0 ppm is contributed by the CH_3 protons of the isopropyl group in *N*-isopropylacrylamide as well as from the CH_3 protons of the methylmethacrylate moiety. The signal peaks at δ 3.8 ppm and δ 3.5 ppm are assigned for the -NCH $(CH_3)_2$ protons of *N*-isopropylacrylamide and the -OCH_3 proton of methylmethacrylate. The broad signal peak from the amidic protons of *N*-isopropylacrylamide can be observed at the downfield region of the spectrum (δ 7.4–8.0 ppm).

Particle Size, Morphology, and Surface Charge of the Polymeric Nanoparticles

The average particle size and the polydispersity index of NMA622 and NVA622 nanoparticles were studied by dynamic light scattering, and only NMA622 is illustrated for sake of brevity. The representative size distribution of the copolymeric nanoparticles is illustrated in Fig. 2B, which clearly shows a narrow size distribution with the average particle diameter of ~80 ± 34 nm and a polydispersity index of 0.119. The size and morphology of the polymeric nanoparticles were further confirmed with transmission electron microscopy (Fig. 2C). Both low-magnification (*right*) and high-magnification (*left*) images shown here show spherical morphology and near-complete homogeneous dispersion of the nanoparticles. The nanoparticle size observed in transmission electron microscopy was consistent with the results obtained by dynamic light scattering. Zeta potential measurements confirmed a comparable negative surface charge for both nanoparticles, specifically −10.3 ± 3.94 for NMA622 and −12.8 ± 3.66 for NVA622.

In vitro Release Kinetics

The *in vitro* release profile of rapamycin from the drug-loaded NMA622 polymeric nanoparticles at “neutral” (pH 7.4) and “acidic” (pH 5.0) is shown in Fig. 2D. A clear distinction is observed for the release kinetics between the two different pH conditions, with an enhanced “burst” effect at the acidic pH within the first 2 hours. Over the next 24 hours, there is increasing parity between the two pH conditions, culminating in ~100% release observed at 168 hours (day 7).

In vivo Pharmacokinetics of NMA622 and NVA622 Compared with Rapamune in Non – Tumor-Bearing Mice

In experiment 1 (Fig. 3A), only trace amounts of rapamycin (<20 ng/mL) were detectable by high-performance liquid chromatography in the plasma of mice receiving free rapamycin in water. In contrast, significant blood levels of rapamycin (~2,500–3,000 ng/mL) were observed with both NMA622- and NVA622-encapsulated nanorapamycin, and no significant difference was apparent in this single time point experiment. The rapamycin concentrations between central venous blood and peripheral blood in experiment 2 (Fig. 3B) were nearly identical at the two sites, confirming equitable systemic distribution of the drug and establishing the validity of using peripheral blood for the time course study in

experiment 3. Figure 3C illustrates the mean rapamcyin blood concentrations for orally administered NMA622- and NVA622-encapsulated rapamycin compared with an equivalent single dose of Rapamune over a 24-hour period. Significant rapamycin blood concentrations were detectable as early as 30 minutes after oral administration, with both nanoparticle formulations. NMA622 displayed a biphasic release/distribution of rapamycin within the first 4 hours after drug administration; this characteristic parallels the *in vitro* release kinetics, as previously described. The mean area under the concentration time curve ($AUC_{0\text{-infinity}}$) was 21,975.7 ng h/mL for NMA622, 11,432.4 ng h/mL for NVA622, and 9536.7 ng h/mL for Rapamune; the differences were not statistically significant due to the large coefficients of variation. The Cp_{max} values were 1,684.9 ng/mL for NMA622, 1,837.9 ng/mL for NVA622, and 580.0 ng/mL for Rapamune, whereas the corresponding T_{max} values were 1.5, 1.33, and 6.67 hours, respectively. There were no significant differences with elimination half-life, clearance, and volume of distribution between the two nanorapamycin formulations (data not shown). In light of the favorable $AUC_{0\text{-infinity}}$ of NMA622 compared with NVA622, all subsequent *in vivo* experiments in mice were done with NMA622 nanoparticles.

Lack of Apparent Systemic Toxicities with Void Oral NMA622 in Mice

Before initiation of treatment studies with oral nanorapamycin, we established the preliminary safety profile of the nanoparticle carrier (NMA622) on longer-term administration than the single-dose experiments described above. Void NMA622 polymeric nanoparticles were administered orally at 500 mg/kg daily to four wild-type CD1 mice (two male, two females) for a period of 4 weeks. No behavioral abnormalities or weight loss was observed during the course of therapy in any of the mice receiving void NMA622 (Fig. 4A). No gross residua of the nanoparticles were seen within the lumen of the gastrointestinal tract, consistent with the biodegradability of the nanoparticles. Histologic examination of major visceral organs (liver, kidney, lung, intestines, etc.) showed no apparent signs of toxicity with NMA622 nanoparticles (Fig. 4B).

Oral Nanorapamycin Inhibits the Growth of Pancreatic Cancer Xenografts

To evaluate the *in vivo* therapeutic efficacy of oral nanorapamycin and to perform a head-to-head comparison with Rapamune, we used a previously described low-passage pancreatic cancer xenograft, Panc198, which is highly sensitive to the injectable rapalogue, temsirolimus (15). Cohorts of athymic mice with s.c. Panc198 xenografts were randomly assigned into one of three arms: PBS only p.o. (control), oral nanorapamycin (NMA622 formulation encapsulating 15 mg/kg equivalent rapamycin), or oral Rapamune (15 mg/kg), administered once daily for 4 weeks. As depicted in Fig. 5A and B, treatment with either oral nanorapamycin or Rapamune resulted in significant growth retardation of s.c. Panc198 xenograft tumors compared with control mice, with significant differences in average tumor volumes observed from weeks 2 through 4. Although the average xenograft volumes were marginally smaller in nanorapamycin-treated mice than in the Rapamune arm, this difference was not statistically significant. We did not observe any behavioral changes, loss of body weight, or other signs of toxicity in oral nanorapamycin–treated mice (Fig. 5C) compared with control or Rapamune-treated mice. The treated and control tumors were harvested at 4 weeks. Growth retardation in oral nanorapamycin – treated Panc198

xenografts was mirrored by histologic changes in the tumor microenvironment, with a more prominent stromal component and smaller tumor cell islands than in control mice (Fig. 5D).

A number of direct and indirect pharmacodynamic assays were also done to confirm the bioavailability of orally delivered rapamycin within the tumor tissues. Mice were euthanized 24 hours after administration of the last oral dose, and blood and xenografted tumors were harvested for rapamycin levels. At this time point, rapamycin was still detectable in both blood and tumor tissues derived from all mice in the nanorapamycin or Rapamune treatment groups but none of the control animals (Fig. 6A). In line with the observed growth inhibition, oral nanorapamycin– and oral Rapamune–treated xenografts showed reduced nuclear Ki67 staining compared with control mice, consistent with reduced proliferation (Fig. 6B). Finally, the status of activation of the mTOR pathway was assessed by immunohistochemistry and by Western blot analysis of control and treated xenografts, using the phosphorylation status of the 40S ribosomal protein S6 kinase (p70s6k) as the readout (20, 21). Both assays showed marked reduction of phospho-p70s6k, but not total p70s6k (Fig. 6C and D), in line with robust mTOR pathway inhibition in oral nanorapamycin– or oral Rapamune–treated Panc198 xenografts.

Discussion

Poor water solubility and low systemic bioavailability are among the more common hurdles that need to be circumvented to translate potential drug candidates into clinical practice (4, 22). Nanoparticle drug delivery strategies that have enabled systemic administration of hydrophobic anticancer drugs include albumin-based nanoparticles of paclitaxel (Abraxane; ref. 23) and liposomal formulations of anthracyclines (DaunoXome and Doxil; refs. 24, 25), all of which are currently approved by the Food and Drug Administration for various cancer indications. Similarly, a number of polymeric micelles or polymer conjugates of hydrophobic drugs have been synthesized (e.g., Genexol-PM, Xyotax, NK911, NK012, etc.) and are at various phases of clinical testing in human cancers (26–28). These examples underscore the great promise of nanotechnology in oncologic therapy. Polymeric materials, in particular, have multiplicity of advantages for *in vivo* drug delivery, including biocompatibility, biodegradability, nonimmunogenicity, active targeting via surface functionalization, and pH-sensitive and thermo-sensitive properties for controlled release in the body (reviewed in refs. 29, 30).

Our laboratory has previously described the synthesis of amphiphilic vinyl polymer–based nanoparticles for encapsulating the hydrophobic plant polyphenol diferuloylmethane (curcumin; ref. 31). The resulting “nanocurcumin” is readily soluble in aqueous media and shows potent growth inhibitory activity against human pancreatic cancer cell lines *in vitro*. In this present study, we extend our prior work to the *in vivo* setting by developing amphiphilic nanoparticles that are capable of delivering the encapsulated drug orally. Specifically, we have engineered nanoparticles composed of *N*-isopropylacrylamide, methylmethacrylate, and acrylic acid in fixed molar ratios of 60:20:20 (designated NMA622) and encapsulated the hydrophobic drug rapamycin within these nanoparticles (nanorapamycin). We have also synthesized an alternate nanoparticle composed of *N*-isopropylacrylamide, vinylpyrrolidone, and acrylic acid in molar ratios of 60:20:20, and

designated these as NVA622. Our choice of the constituent monomers was not random, but rather guided by the need for developing a mucoadhesive polymer that would “stick” to the gastrointestinal tract mucosa during transit. Previous experimental attempts at developing orally bioavailable nanoparticles for drug, peptide, or gene delivery have highlighted the importance of the role played by the nanoparticle surface charge and hydrophilicity/hydrophobicity ratio in increasing gastrointestinal transit time, and thereby enhancing mucosal transcytosis (reviewed in refs. 32, 33). One common strategy for promoting oral uptake has been surface modification with polyethylene glycol (PEG), which provides negative surface charge and hydrophilicity, rendering the particles mucoadhesive and increasing transit times in the gastrointestinal tract (34). The incorporation of acrylic acid in our copolymer provides analogous negative carboxylic groups, as well as hydrophilicity, thus obviating the need for “PEGylation.” Although we did not perform quantitative fluorescence trafficking studies on our nanoparticles across the gut mucosa, one can speculate that the superior pharmacokinetics of NMA622 compared with NVA622 might be a consequence of a better hydrophilic/hydrophobic ratio due to the incorporation of hydrophobic methylmethacrylate in the copolymer in combination with the negative charge provided by the carboxylic moieties of acrylic acid.

In this study, we have successfully shown the ability of single-agent oral nanorapamycin to significantly inhibit the growth of pancreatic cancer xenografts in mice over a 4-week once-daily regimen. Further, we have confirmed that this growth inhibition is accompanied by blockade in activation of the mTOR pathway, which is the molecular target of the encapsulated therapeutic (9). Rapamycin is a prototype for a poorly water-soluble drug with low oral bioavailability that would greatly benefit from nanoencapsulation of the type described in this report. Several strategies have been used to improve the pharmacokinetics of rapamycin, including the development of water-soluble analogues like temsirolimus (CCI-779), deforolimus (AP23573), and everolimus (RAD001), which can be administered through either i.v. or oral routes, and are actively undergoing evaluation in a variety of human cancers (35–38). The parental compound (sirolimus) itself has been rendered orally bioavailable by fine milling (grinding) of the crystalline drug to particles <400 nm in size, using a proprietary “NanoCrystal” technology (Rapamune), which increases the exposed surface area of the ingested drug and enhances absorption in the gastrointestinal tract (39, 40). Finally, a parenteral-only albumin nanoparticle (nab) formulation of rapamycin (ABI-009) is undergoing phase I trial in solid and hematologic malignancies (41). In the current study, we performed a direct comparison between Rapamune and NMA622 particles vis-à-vis *in vivo* pharmacokinetics and therapeutic efficacy in a pancreatic cancer xenograft model. We were able to demonstrable a superior pharmacokinetic disposition of NMA622 over Rapamune, although both formulations had essentially similar growth inhibitory effects on the Panc198 xenograft model. Given the exquisite sensitivity of this xenograft to mTOR inhibition (14, 15), the comparable antitumor efficacy is not unexpected, and future studies in more recalcitrant solid tumor models will show whether the enhanced systemic bioavailability translates into superior efficacy.

In addition to the oral bioavailability and demonstrable *in vivo* preclinical efficacy, there are several encouraging caveats to nanorapamycin vis-à-vis the existing formulations. First, the

polymeric nanoparticles we have synthesized are consistently smaller than 100 nm in diameter, which, combined with their intrinsic mucoadhesive character, should facilitate oral uptake that is at least comparable, if not superior, to the larger rapamycin nanocrystals. As the time course experiments show, significant blood rapamycin levels are observed as early as 30 minutes after oral administration of nanorapamycin, and the drug continues to be detectable in blood 24 hours after the last dose. Second, the drug-loaded nanorapamycin is lyophilized and stored in powder form at room temperature, from which it can be readily reconstituted in aqueous media for parenteral administration or dispensed as measured modules for oral intake (e.g., as capsules). For example, the NMA622 formulation used for preclinical studies was synthesized as much as 2 to 3 months before oral administration without demonstrable loss of efficacy. Thus, from a logistical perspective, nanorapamycin offers significant advantages over a parenteral-only formulation or one that requires refrigeration for storage and transport. Third, incidental toxicity resulting from the nanoparticulate carrier is an issue of considerable concern to regulatory agencies as well as to the medical community (42). Our preliminary experiments with NMA622 nanoparticles show that even “mega” dosing of the void polymers (500 mg/kg daily p.o.) for 4 weeks in mice failed to elicit any apparent systemic toxicities; however, we emphasize that further toxicity studies are clearly needed to cement this finding. Finally, although not a focus of this current study, the polymeric nanoparticles can be surface modified by conjugation of peptides, aptamers, or antibodies to reactive carboxylic groups for enabling active targeting to specific cell types *in vivo*. As our own tumor treatment data exemplify, active targeting to cancer tissues is by no means mandatory, and the nanoparticles likely accumulate in the peritumoral milieu as a result of the so-called “enhanced permeability and retention” effect (43). Nevertheless, active targeting might significantly decrease the effective dosing required for antitumor efficacy. For example, MacDiarmid et al. (44, 45) reported that they were able to reduce i.v. doxorubicin doses required to achieve significant growth inhibition of murine breast cancer xenografts by more than 3 log scales when the drug was encapsulated in so-called “nanocells” coated with anti–epidermal growth factor receptor antibodies. Our group has previously identified several cell surface antigens preferentially overexpressed on pancreatic cancer (46) and has recently confirmed the feasibility of delivering antibody-conjugated radionuclides and nanoparticles targeted to these surface antigens (47, 48).

In conclusion, we report the synthesis, physicochemical characterization, and preliminary toxicity studies of polymeric nanoparticles capable of delivering hydrophobic drugs through the oral route. We have shown the *in vivo* therapeutic efficacy of an oral nanorapamycin formulation using pancreatic cancer xenografts as a disease model. In addition to rapamycin, we have encapsulated a broad range of hydrophobic agents against cancer and other nonneoplastic diseases (e.g., paclitaxel, curcumin, rifampicin, griseofulvin, etc.) in our polymeric nanoparticles (Supplementary Fig. S1), and the application of these nano-drug formulations in relevant disease models is presently ongoing in our laboratory. We envision that the development of a robust and safe oral nano-delivery platform will enable the systemic administration of compounds otherwise not amenable to this delivery route and will improve patient compliance and reduce adverse events.

Acknowledgments

Grant support: The Sol Goldman Pancreatic Cancer Research Center (A. Maitra), a fellowship grant within the postdoctoral program of the German Academic Exchange Service (DAAD; G. Feldmann), the Dutch Cancer Foundation KWF (Koningin Wilhelmina Fonds; J-B.M. Koorstra), and NIH grant P30CA069773 (M.A. Rudek).

References

1. Lindenberg M, Kopp S, Dressman JB. Classification of orally administered drugs on the World Health Organization Model List of Essential Medicines according to the biopharmaceutics classification system. Eur J Pharm Biopharm. 2004; 58:265–278. [PubMed: 15296954]
2. Shepherd GM. Hypersensitivity reactions to chemotherapeutic drugs. Clin Rev Allergy Immunol. 2003; 24:253–262. [PubMed: 12721396]
3. ten Tije AJ, Verweij J, Loos WJ, Sparreboom A. Pharmacological effects of formulation vehicles: implications for cancer chemotherapy. Clin Pharmacokinet. 2003; 42:665–685. [PubMed: 12844327]
4. Heath JR, Davis ME. Nanotechnology and cancer. Annu Rev Med. 2008; 59:251–265. [PubMed: 17937588]
5. von Pawel J, Gatzemeier U, Pujol JL, et al. Phase ii comparator study of oral versus intravenous topotecan in patients with chemosensitive small-cell lung cancer. J Clin Oncol. 2001; 19:1743–1749. [PubMed: 11251005]
6. Borner MM, Schoffski P, de Wit R, et al. Patient preference and pharmacokinetics of oral modulated UFT versus intravenous fluorouracil and leucovorin: a randomised crossover trial in advanced colorectal cancer. Eur J Cancer. 2002; 38:349–358. [PubMed: 11818199]
7. Findlay M, von Minckwitz G, Wardley A. Effective oral chemotherapy for breast cancer: pillars of strength. Ann Oncol. 2008; 19:212–222. [PubMed: 18006898]
8. Ward SE, Kaltenthaler E, Cowan J, Marples M, Orr B, Seymour MT. The clinical and economic benefits of capecitabine and tegafur with uracil in metastatic colorectal cancer. Br J Cancer. 2006; 95:27–34. [PubMed: 16804526]
9. Easton JB, Houghton PJ. mTOR and cancer therapy. Oncogene. 2006; 25:6436–6446. [PubMed: 17041628]
10. Averous J, Proud CG. When translation meets transformation: the mTOR story. Oncogene. 2006; 25:6423–6435. [PubMed: 17041627]
11. Aissat N, Le Tourneau C, Ghoul A, et al. Antiproliferative effects of rapamycin as a single agent and in combination with carboplatin and paclitaxel in head and neck cancer cell lines. Cancer Chemother Pharmacol. 2008; 62:305–313. [PubMed: 17912526]
12. Settleman J, Kurie JM. Drugging the bad “AKT-TOR” to overcome TKI-resistant lung cancer. Cancer Cell. 2007; 12:6–8. [PubMed: 17613432]
13. Napoli KL, Wang ME, Stepkowski SM, Kahan BD. Distribution of sirolimus in rat tissue. Clin Biochem. 1997; 30:135–142. [PubMed: 9127695]
14. Rubio-Viqueira B, Jimeno A, Cusatis G, et al. An *in vivo* platform for translational drug development in pancreatic cancer. Clin Cancer Res. 2006; 12:4652–4661. [PubMed: 16899615]
15. Rubio-Viqueira B, Mezzadra H, Nielsen ME, et al. Optimizing the development of targeted agents in pancreatic cancer: tumor fine-needle aspiration biopsy as a platform for novel prospective *ex vivo* drug sensitivity assays. Mol Cancer Ther. 2007; 6:515–523. [PubMed: 17308050]
16. Dong J, Feldmann G, Huang J, et al. Elucidation of a universal size-control mechanism in *Drosophila* and mammals. Cell. 2007; 130:1120–1133. [PubMed: 17889654]
17. Vicente FB, Smith FA, Peng Y, Wang S. Evaluation of an immunoassay of whole blood sirolimus in pediatric transplant patients in comparison with high-performance liquid chromatography/tandem mass spectrometry. Clin Chem Lab Med. 2006; 44:497–499. [PubMed: 16599847]
18. Wang S, Magill JE, Vicente FB. A fast and simple high-performance liquid chromatography/mass spectrometry method for simultaneous measurement of whole blood tacrolimus and sirolimus. Arch Pathol Lab Med. 2005; 129:661–665. [PubMed: 15859639]

19. Feldmann G, Dhara S, Fendrich V, et al. Blockade of hedgehog signaling inhibits pancreatic cancer invasion and metastases: a new paradigm for combination therapy in solid cancers. Cancer Res. 2007; 67:2187–2196. [PubMed: 17332349]
20. Hidalgo M, Rowinsky EK. The rapamycin-sensitive signal transduction pathway as a target for cancer therapy. Oncogene. 2000; 19:6680–6686. [PubMed: 11426655]
21. Ruvinsky I, Meyuhas O. Ribosomal protein S6 phosphorylation: from protein synthesis to cell size. Trends Biochem Sci. 2006; 31:342–348. [PubMed: 16679021]
22. Langer R. Drug delivery and targeting. Nature. 1998; 392:5–10. [PubMed: 9579855]
23. Henderson IC, Bhatia V. Nab-paclitaxel for breast cancer: a new formulation with an improved safety profile and greater efficacy. Expert review of anticancer therapy. 2007; 7:919–943. [PubMed: 17627452]
24. Gabizon AA, Shmeeda H, Zalipsky S. Pros and cons of the liposome platform in cancer drug targeting. J Liposome Res. 2006; 16:175–183. [PubMed: 16952872]
25. Alberts DS, Muggia FM, Carmichael J, et al. Efficacy and safety of liposomal anthracyclines in phase I/II clinical trials. Semin Oncol. 2004; 31:53–90. [PubMed: 15717738]
26. Kim DW, Kim SY, Kim HK, et al. Multicenter phase II trial of Genexol-PM, a novel Cremophor-free, polymeric micelle formulation of paclitaxel, with cisplatin in patients with advanced non-small-cell lung cancer. Ann Oncol. 2007; 18:2009–2014. [PubMed: 17785767]
27. Matsumura Y. Poly (amino acid) micelle nanocarriers in preclinical and clinical studies. Adv Drug Deliv Rev. 2008; 60:899–914. [PubMed: 18406004]
28. Boddy AV, Plummer ER, Todd R, et al. A phase I and pharmacokinetic study of paclitaxel poliglumex (XYOTAX), investigating both 3-weekly and 2-weekly schedules. Clin Cancer Res. 2005; 11:7834–7840. [PubMed: 16278406]
29. Nahar M, Dutta T, Murugesan S, et al. Functional polymeric nanoparticles: an efficient and promising tool for active delivery of bioactives. Crit Rev Ther Drug Carrier Systems. 2006; 23:259–318.
30. Pridgen EM, Langer R, Farokhzad OC. Biodegradable, polymeric nanoparticle delivery systems for cancer therapy. Nanomed. 2007; 2:669–680.
31. Bisht S, Feldmann G, Soni S, et al. Polymeric nanoparticle-encapsulated curcumin ("nanocurcumin"): a novel strategy for human cancer therapy. J Nanobiotechnol. 2007; 5:3.
32. Damge C, Reis CP, Maincent P. Nanoparticle strategies for the oral delivery of insulin. Expert Opin Drug Deliv. 2008; 5:45–68. [PubMed: 18095928]
33. Bhavsar MD, Amiji MM. Polymeric nano- and microparticle technologies for oral gene delivery. Expert Opin Drug Deliv. 2007; 4:197–213. [PubMed: 17489649]
34. Yoncheva K, Gomez S, Campanero MA, Gamazo C, Irache JM. Bioadhesive properties of pegylated nanoparticles. Expert Opin Drug Deliv. 2005; 2:205–218. [PubMed: 16296748]
35. Ma WW, Jimeno A. Temsirolimus. Drugs Today (Barc). 2007; 43:659–669. [PubMed: 17987219]
36. Rubio-Viqueira B, Hidalgo M. Targeting mTOR for cancer treatment. Curr Opin Investig Drugs. 2006; 7:501–512.
37. Smolewski P. Recent developments in targeting the mammalian target of rapamycin (mTOR) kinase pathway. Anticancer Drugs. 2006; 17:487–494. [PubMed: 16702804]
38. Mita MM, Mita AC, Chu QS, et al. Phase I trial of the novel mammalian target of rapamycin inhibitor deforolimus (AP23573; MK-8669) administered intravenously daily for 5 days every 2 weeks to patients with advanced malignancies. J Clin Oncol. 2008; 26:361–367. [PubMed: 18202410]
39. Muller RH, Keck CM. Challenges and solutions for the delivery of biotech drugs—a review of drug nanocrystal technology and lipid nanoparticles. J Biotechnol. 2004; 113:151–170. [PubMed: 15380654]
40. Wagner V, Dullaart A, Bock AK, Zweck A. The emerging nanomedicine landscape. Nat Biotechnol. 2006; 24:1211–1217. [PubMed: 17033654]
41. Hawkins MJ, Soon-Shiong P, Desai N. Protein nanoparticles as drug carriers in clinical medicine. Adv Drug Deliv Rev. 2008; 60:876–885. [PubMed: 18423779]

42. Hoet PH, Bruske-Hohlfeld I, Salata OV. Nanoparticles—known and unknown health risks. J Nanobiotechnol. 2004; 2:12.

43. Greish K. Enhanced permeability and retention of macromolecular drugs in solid tumors: a royal gate for targeted anticancer nanomedicines. J Drug Target. 2007; 15:457–464. [PubMed: 17671892]

44. MacDiarmid JA, Madrid-Weiss J, Amaro-Mugridge NB, Phillips L, Brahmbhatt H. Bacterially-derived nanocells for tumor-targeted delivery of chemotherapeutics and cell cycle inhibitors. Cell Cycle Georgetown TX. 2007; 6:2099–2105.

45. MacDiarmid JA, Mugridge NB, Weiss JC, et al. Bacterially derived 400 nm particles for encapsulation and cancer cell targeting of chemotherapeutics. Cancer Cell. 2007; 11:431–445. [PubMed: 17482133]

46. Maitra A, Hruban RH. Pancreatic cancer. Annual review of pathology. 2008; 3:157–188.

47. Foss CA, Fox JJ, Feldmann G, et al. Radiolabeled anti-claudin 4 and anti-prostate stem cell antigen: initial imaging in experimental models of pancreatic cancer. Mol Imaging. 2007; 6:131–139. [PubMed: 17445507]

48. Qian J, Yong KT, Roy I, et al. Imaging pancreatic cancer using surface-functionalized quantum dots. J Phys Chem. 2007; 111:6969–6972.

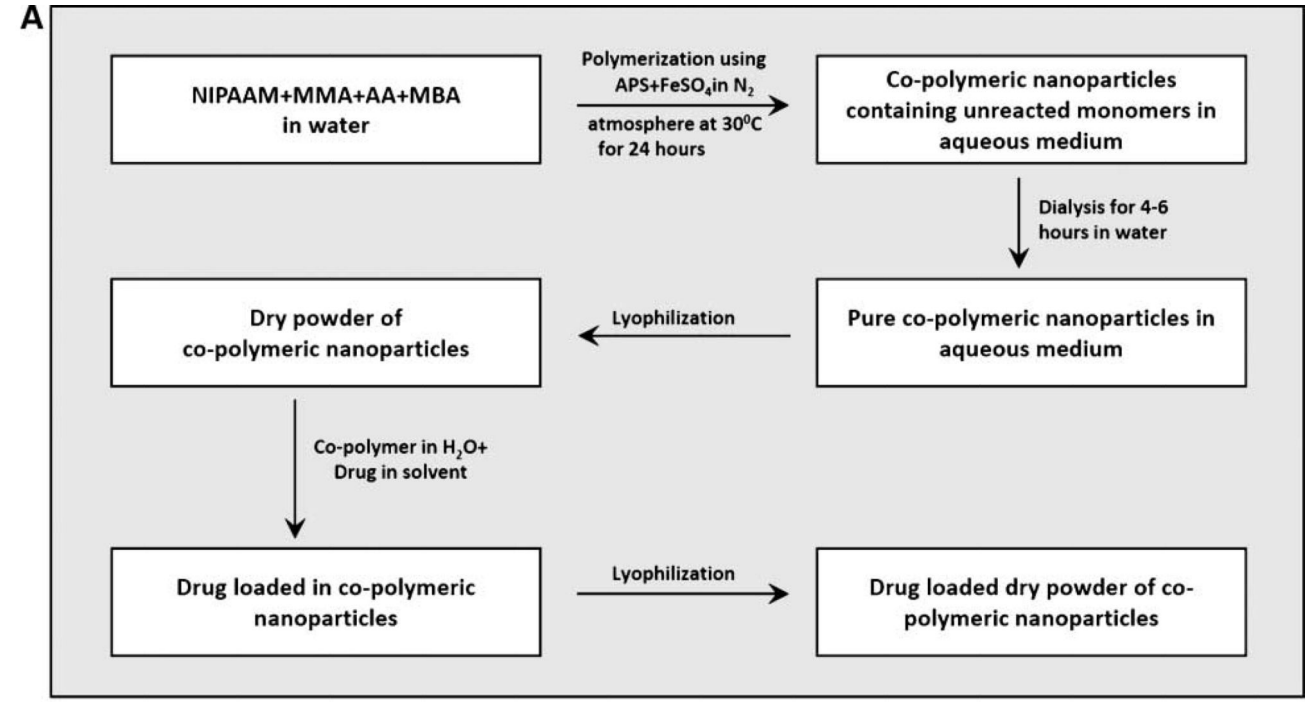

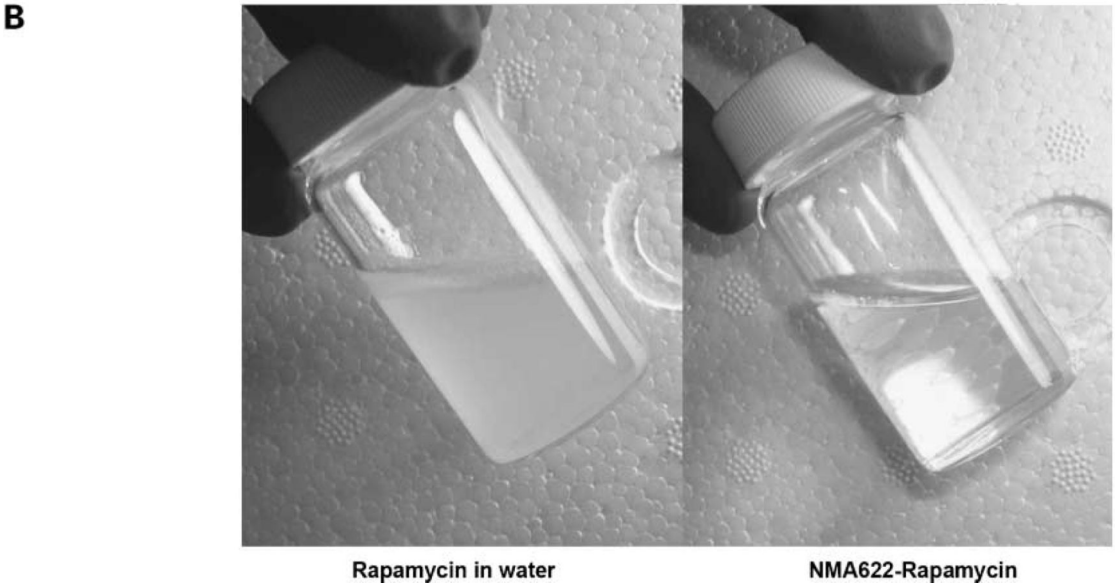

Figure 1.

Synthesis of NMA622 and NVA622 polymeric nanoparticles. **A**, schematic overview of the synthetic procedure for NMA622 copolymeric nanoparticles. *NIPAAM*, *N*-isopropylacrylamide; *MMA*, methylmethacrylate; *AA*, acrylic acid; *MBA*, *N*,*N*′-methylene-bis-acrylamide; *APS*, ammonium persulfate. A homologous scheme is used for synthesis of NVA622 nanoparticles. **B**, nanoencapsulation of rapamycin in NMA622 copolymeric nanoparticles leads to complete dispersion of the drug in aqueous media. Free rapamycin

suspended in water results in a turbid solution (*left*), whereas a transparent solution is seen with NMA622-encapsulated rapamycin (*right*).

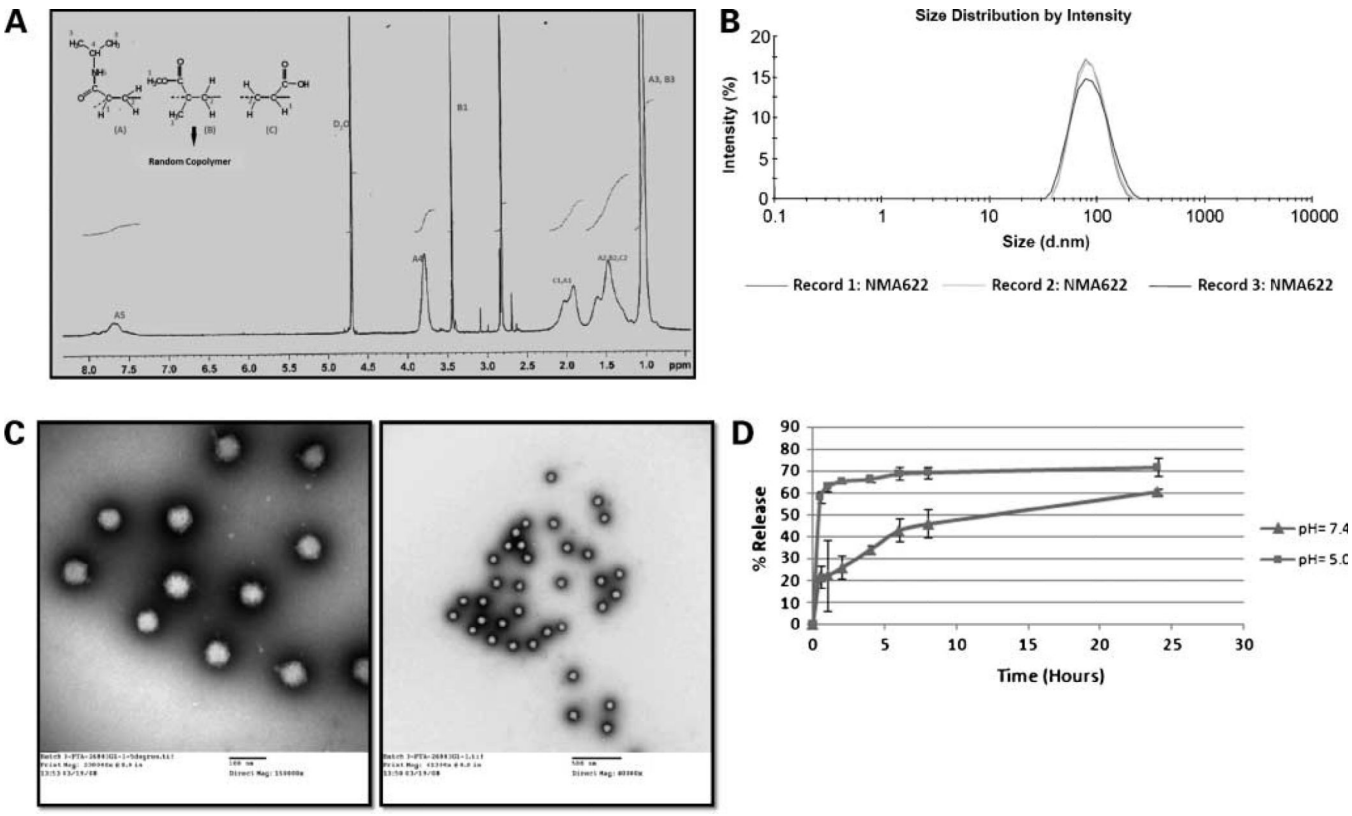

Figure 2.

Physicochemical characterization of NMA622 polymeric nanoparticles. **A**, spectroscopic measurement shows complete polymerization and absence of the monomers, as is evident by the ^{1}H nuclear magnetic resonance spectrum. **B**, representative size distribution overlay with dynamic light scattering shows the average diameter of the particles to be ~80 ± 34 nm, with a polydispersity index of 0.119. **C**, transmission electron microscopy is used to determine the size and morphology of the copolymeric nanoparticles. The figures confirm that the nanoparticles are completely spherical, with low polydispersity and an average diameter of <100 nm (*left*, × 150,000 magnification; *right*, ×40,000 magnification). **D**, *in vitro* release kinetics of rapamycin from NMA622 polymeric nanoparticles dispersed at pH 7.4 (*triangles*) and pH 5.0 (*squares*) shows a first sudden burst release of the drug within 30 min at the acidic pH. *Points*, mean of experiments done in triplicates; *bars*, SD.

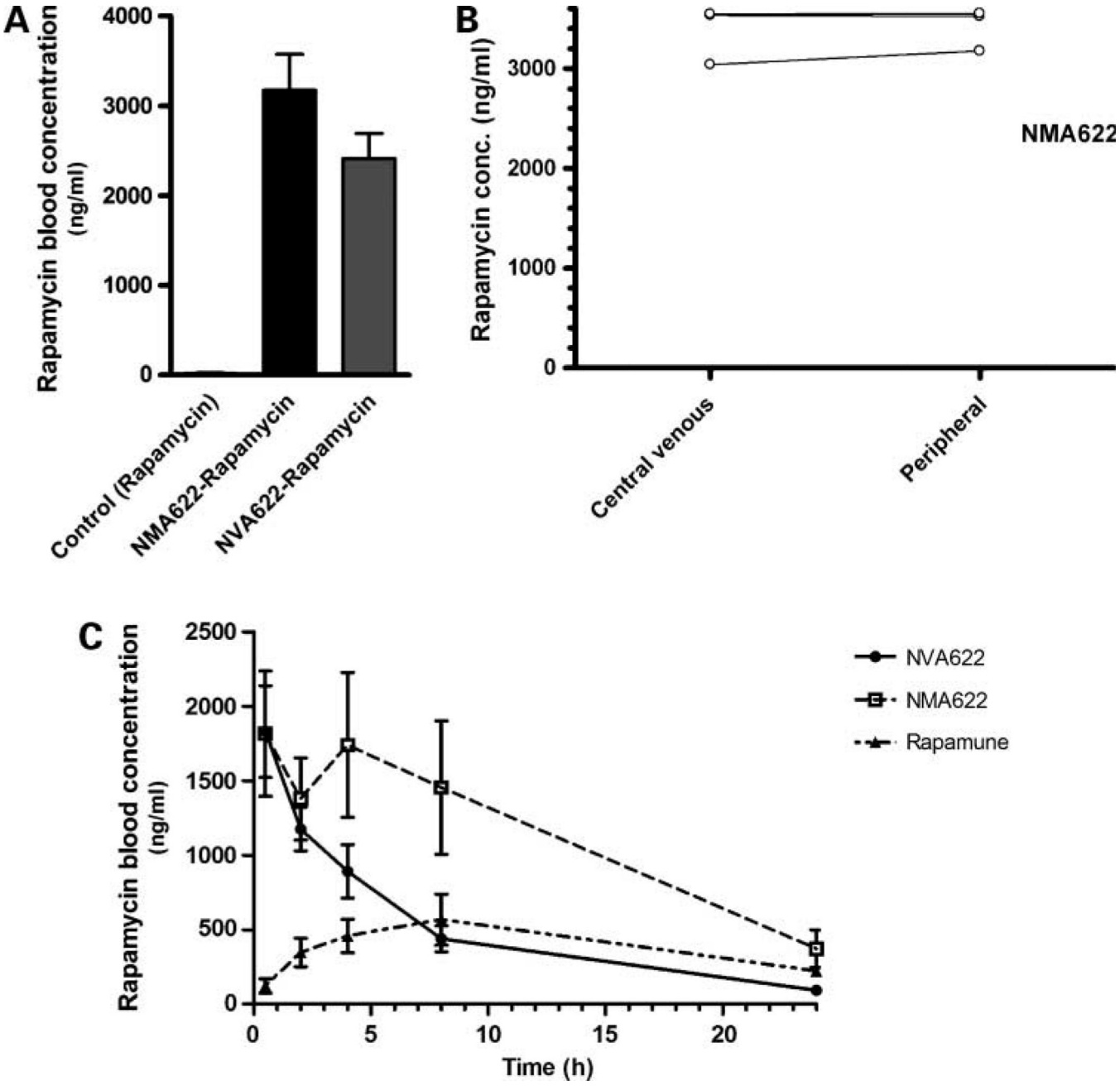

Figure 3.

In vivo pharmacokinetics of orally administered NMA622 and NVA622 nanoparticles. **A**, rapamycin whole blood concentrations were measured in central blood obtained via cardiac puncture 2 h after oral application of rapamycin (15 mg/kg) administered in either NMA622 or NVA622 (n = 4 per arm). Rapamycin suspended in water was used as control. *Y axis*, mean rapamycin concentrations (ng/mL) determined by high-performance liquid chromatography. **B**, rapamycin concentrations were compared at 2 h after oral administration in central versus peripheral venous blood specimens in three mice administered single dose of NMA622-encapsulated rapamycin (15 mg/kg). *Y axis*, mean

rapamycin concentrations (ng/mL) determined by high-performance liquid chromatography. **C**, concentrations of rapamycin were determined at 30 min and at 2, 4, 8, and 24 h after oral administration of a single dose of rapamycin encapsulated in NMA622 or NVA622 nanoparticles, and compared with that of orally administered Rapamune (all equivalent to 15 mg/kg of active compound). Peripheral blood was obtained for this time course experiment from six mice per cohort. Please see text for details of pharmacokinetic parameters for each of the three formulations.

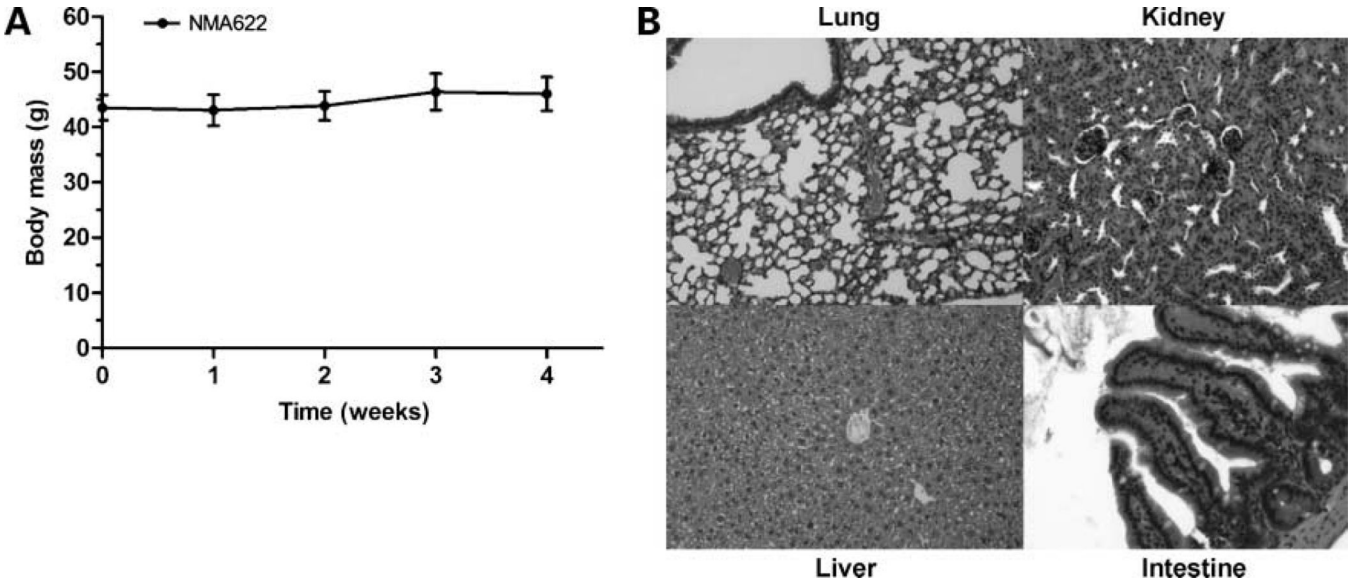

Figure 4.

Toxicity profile of void NMA622 nanoparticles administered over 4 wk. **A**, treatment with void NMA622 nanoparticles (500 mg/kg p.o.) for 4 wk did not lead to weight loss in wild-type CD1 mice (n = 4 per group) at any time during the course of therapy. **B**, representative photomicrographs of lung, kidney, liver, and intestines (H&E staining). No evidence of toxicities was discernible in these organs.

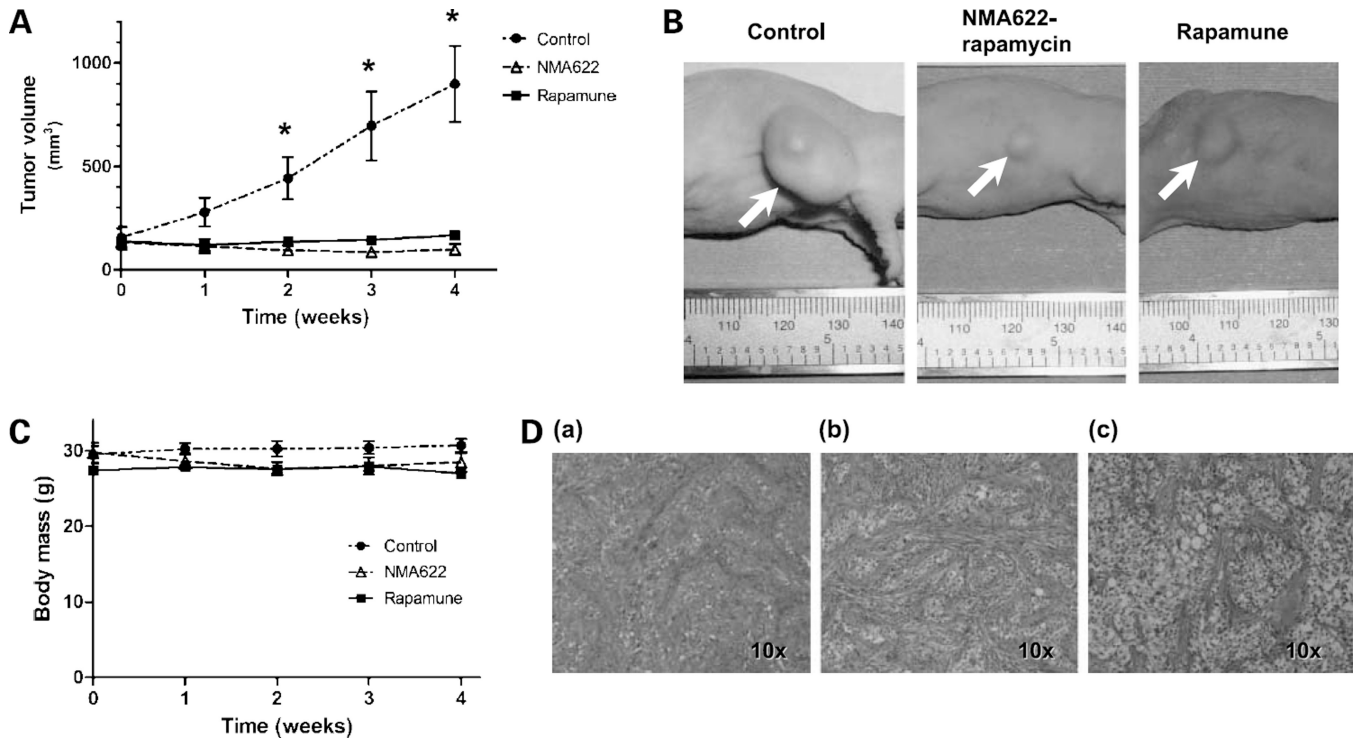

Figure 5.

In vivo efficacy of oral nanorapamycin and oral Rapamune in the rapalogue-sensitive Panc198 pancreatic cancer xenograft. **A**, treatment of the s.c. Panc198 xenografts with oral nanorapamycin and oral Rapamune results in significant growth inhibition as compared with mock-treated controls. *X axis*, weeks of therapy; *Y axis*, average tumor volumes for each time point of measurement (seven Panc198 xenografts per arm). **B**, representative photographs of Panc198 xenograft–bearing mice treated with oral nanorapamycin, oral Rapamune, and control tumor, taken at the end of the 4-wk treatment course. **C**, no loss of body weight was observed in mice in the oral nanorapamycin treatment arm, comparable to the Rapamune and control arms, underscoring the absence of incidental toxicities. **D**, representative photomicrographs of control (*a*), NMA622-nanorapamycin–treated (*b*), or Rapamune-treated (*c*) Panc198 xenografts. There is an increase in the intervening stromal component, and smaller islands of neoplastic cells are seen, in the xenografts receiving oral nanorapamycin compared with control xenografts; this alteration was less appreciable in the Rapamune group.

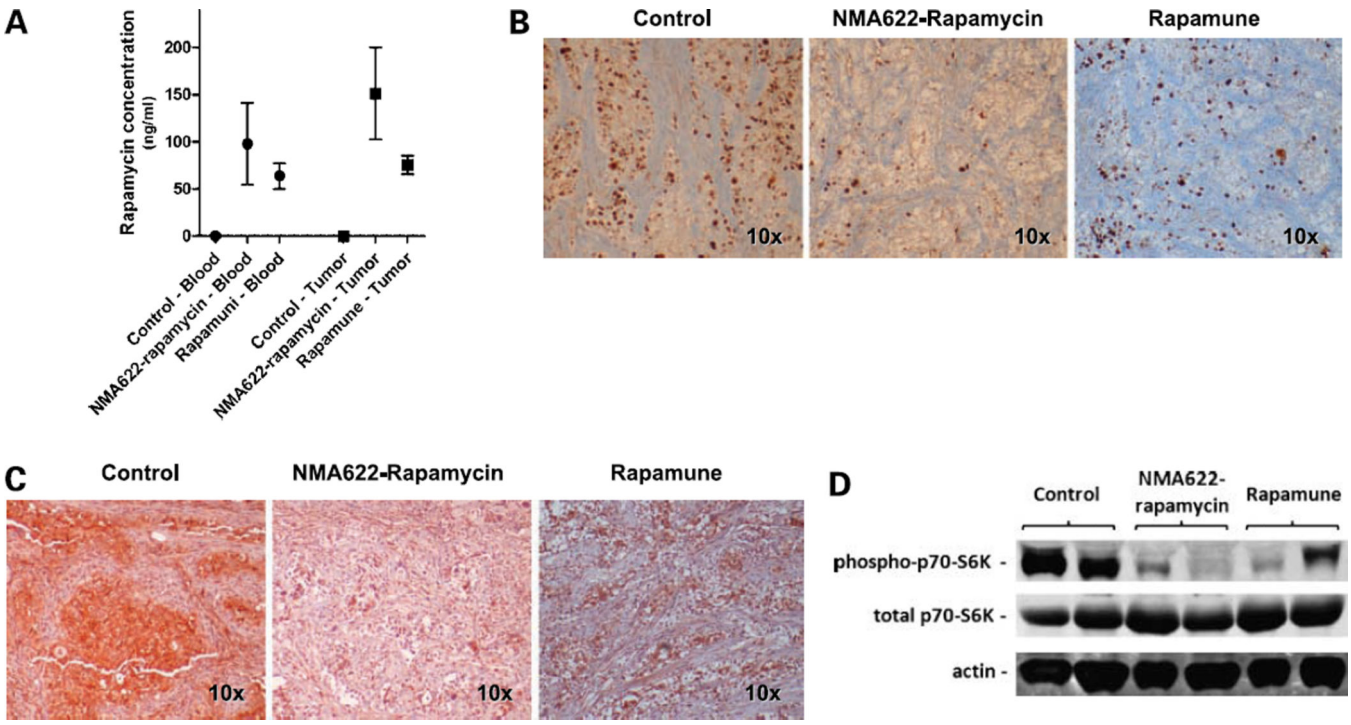

Figure 6.

Oral nanorapamycin accumulates within tumor tissues, blocks proliferation, and inhibits the mTOR signaling pathway in pancreatic cancer xenografts. **A**, twenty-four hours after administration of the last oral nanorapamycin and Rapamune dose, rapamycin concentrations were measured in blood as well as in tumor tissue samples by high-performance liquid chromatography. *Y axis*, average concentrations (ng/mL) of rapamycin in plasma obtained from four treated mice in each arm and in tissue samples from seven treated xenografts. *Points*, mean; *bars*, SE. **B**, treatment with oral nanorapamycin and Rapamune leads to impaired tumor cell proliferation, as shown by immunohistochemistry for Ki67 (MIB-1) nuclear antigen, compared with levels in control xenografts. **C**, oral nanorapamycin inhibits the mTOR signaling pathway in Panc198 xenografts, as evidenced by marked downregulation of the phosphorylated form of p70s6k, as determined by immunohistochemistry on formalin-fixed xenograft tissues. Comparable inhibition is observed with Rapamune therapy. **D**, oral nanorapamycin inhibits the mTOR signaling pathway in Panc198 xenografts, as evidenced by marked downregulation of the phosphorylated form of p70s6k, determined by Western blot analysis of frozen xenograft tissues. Comparable inhibition is observed with Rapamune therapy.